AD-A187 334 VELOCITY MEASUREMENTS IN A 3D (THREE DIMENSIONAL) SHOCK 1/1
WAVE LAMINAR BOUN..(U) VON KARMAN INST FOR FLUID
DYNAMICS RHODE-SAINT-GENESE (BELGIU.. G DECONINCK ET AL.
UNCLASSIFIED 31 JUL 87 VKI-CR8734AN AFOSR-TR-87-1388 F/G 20/4 NL

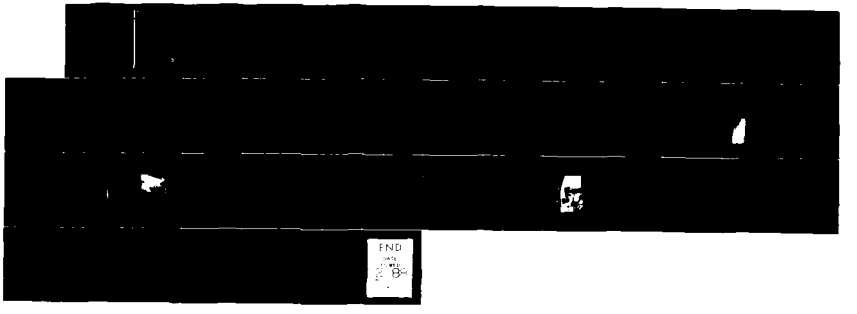

END

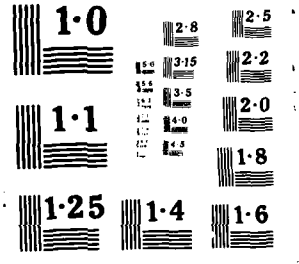
1·0
1·1
1·25
1·4
1·6
1·8
2·0
2·2
2·5
2·8
3·15
3·5
4·0
4·5

AFOSR-TR- 87-1388

Grant AFOSR 83-0273

VELOCITY MEASUREMENTS IN A 3D SHOCK WAVE LAMINAR BOUNDARY LAYER INTERACTION

G. DEGREZ & J.J. GINOUX

von Karman Institute for Fluid Dynamics
Chaussée de Waterloo, 72
B - 1640 Rhode Saint Genèse - Belgium

July 31, 1987

FINAL SCIENTIFIC REPORT
01 August 1985 - 31 July 1986

Prepared for

AFOSR/PKN Bolling AFB DC 20332
and
European Office of Aerospace Research and Development
London, UK

SECURITY CLASSIFICATION OF THIS PAGE (When Data Entered)

UNCLASSIFIED

REPORT DOCUMENTATION PAGE

READ INSTRUCTIONS BEFORE COMPLETING FORM

1. REPORT NUMBER AFOSR-TR- 87-1388	2. GOVT ACCESSION NO.
3. RECIPIENT'S CATALOG NUMBER	
4. TITLE (and Subtitle) VELOCITY MEASUREMENTS IN A 3D SHOCK WAVE - LAMINAR BOUNDARY LAYER INTERACTION	5. TYPE OF REPORT & PERIOD COVERED Final Scientific Report 01 Aug. 85 - 31 Jul. 86
	6. PERFORMING ORG. REPORT NUMBER CR8734AR
7. AUTHOR(s) G. DEGREZ & J.J. GINOUX	8. CONTRACT OR GRANT NUMBER(s) AFOSR 83-0273
9. PERFORMING ORGANIZATION NAME AND ADDRESS von Karman Institute for Fluid Dynamics Chaussée de Waterloo, 72 B - 1640 Rhode Saint Genèse - Belgium	10. PROGRAM ELEMENT, PROJECT, TASK AREA & WORK UNIT NUMBERS 61102F 2307/A1
11. CONTROLLING OFFICE NAME AND ADDRESS Air Force Office of Scientific Research/NA Bolling AFB, DC 20332-6448	12. REPORT DATE 31 July 1987
	13. NUMBER OF PAGES 45
14. MONITORING AGENCY NAME & ADDRESS (if different from Controlling Office) European Office of Aerospace Research and Development/LDV Box 14 FPO New York 09510-0200	15. SECURITY CLASS. (of this report)
	15a. DECLASSIFICATION/DOWNGRADING SCHEDULE

16. DISTRIBUTION STATEMENT (of this Report)

Approved for public release;
Distribution unlimited

17. DISTRIBUTION STATEMENT (of the abstract entered in Block 20, if different from Report)

18. SUPPLEMENTARY NOTES

19. KEY WORDS (Continue on reverse side if necessary and identify by block number)

Two and three dimensional compressible viscous flow
Laminar boundary layer - separation
Shock wave - boundary layer interaction
Laser doppler velocimetry

20. ABSTRACT (Continue on reverse side if necessary and identify by block number)

An experimental investigation of the three dimensional laminar boundary layer separation associated with an incident swept shock wave was conducted in the von Karman Institute (VKI) S-1 supersonic wind tunnel operating at Mach 2.15. Mean velocity profiles were measured both in the attached separated and reattachment flow regions using a laser doppler velocimeter. A comparison of the measurements with a full 3D Navier-Stokes solver, developed at the VKI, exhibited good agreement in all three regions, thus validating the code which was based on the Beam-Warming algorithm. The report also reviews the earlier parts of the Grant dealing with a) the necessary developments in LDV to achieve high quality data and b) the study of the 2D shock boundary layer interaction.

DD FORM 1 JAN 73 1473 EDITION OF 1 NOV 65 IS OBSOLETE

UNCLASSIFIED

SECURITY CLASSIFICATION OF THIS PAGE (When Data Entered)

Grant AFOSR 83-0273

VELOCITY MEASUREMENTS IN A 3D SHOCK WAVE LAMINAR BOUNDARY LAYER INTERACTION

G. DEGREZ & J.J. GINOUX

von Karman Institute for Fluid Dynamics
Chaussée de Waterloo, 72
B - 1640 Rhode Saint Genèse - Belgium

July 31, 1987

FINAL SCIENTIFIC REPORT
01 August 1985 - 31 July 1986

Prepared for

AFOSR/PKN Bolling AFB DC 20332
and
European Office of Aerospace Research and Development
London, UK

TABLE OF CONTENTS

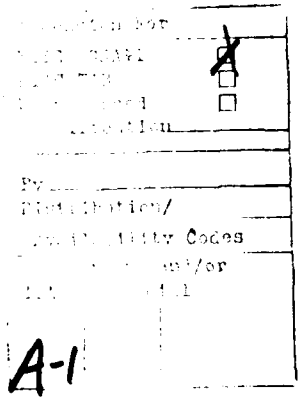

LIST OF SYMBOLS

L_{SH} - coordinate along inviscid shock; (see Fig. 3).

M - Mach number

P - pressure

Re - Reynolds number

S - coordinate normal to inviscid shock

T - temperature

U_{mean} - mean velocity determined from a histogram

U_{peak} - maximum velocity on a histogram

X,Y Coordinates for 2D interaction

X - same

Y - Coordinate normal to plate

X,Y,Z Coordinates for 3D interaction; see (Fig. 3)

X - Coordinate in free-stream flow direction

Y - Coordinate in plane of plate

Z - Coordinate normal to plate

X_F - distance from leading edge of plate to wedge approx., 3D interaction; (see Fig. 3).

X_{SH} - distance from leading edge to shock interaction location 2D interaction; (see Fig. 1).

α - wedge angle (6°)

σ - standard deviation

SUBSCRIPTS

∞ - free stream conditions

o - conditions upstream of interaction

e - conditions at outer edge of boundary layer

t - total conditions

LIST OF FIGURES

14. Histogram deep within attached boundary layer showing influence of amplitude limiter.

15a. Raw data : Station 1. Peak velocity.

15b. Corrected data : Station 1. Peak velocity.

15c. Raw data : Station 1. Mean velocity.

15d. Corrected data : Station 1. Mean velocity.

16a. Raw data : Station 2. Peak velocity.

16b. Corrected data : Station 2. Peak velocity and mean velocity.

17. Corrected data : Station 3. Peak velocity and mean velocity.

1. INTRODUCTION

Three dimensional (3D) shock wave boundary layer interactions constitute a problem of fluid mechanics which has received extensive attention over the last decade [1-5]. Despite this attention, many physical mechanisms remain poorly understood. To aid in the resolution of this problem, the von Karman Institute has undertaken a series of studies concerning the 3D skewed shock wave laminar boundary layer interaction. In addition to their own significance, experimental data for such a problem also provide a test case for comparison with Navier-Stokes calculations which is free of the uncertainties associated with turbulence modeling.

First, surface flow data were collected and analysed under Grant AFOSR 82-0051 [5 & 6]. This research showed the existence of a large region of separated flow and proved that the three dimensional skewed shock wave laminar interaction could be correlated by a functional form similar to turbulent correlations.

Surface flow data provide only partial information on the flow field. In addition, velocity distributions are required, particularly as they constitute the most critical feature for the comparison of numerical solutions. Obtaining these velocity distributions represents a mojor experimental challenge because of the combination of high speed, three dimensionality, the need for high spatial resolution and the proximity of solid surfaces. Laser doppler velocimetry (LDV) was selected as the technique best suited to overcome these difficulties.

A step by step approach to the high speed 3D problem was outlined in the original proposal. In the first step [7], the problems caused by the need for high spatial resolution and the proximity of solid surfaces were addressed and solved by studying the laminar separated flow over an elliptic cylinder.

In the second step, the problem of high speed was added to the previous ones. The flow studied was the two dimensional incident shock wave laminar boundary layer interaction. Despite it being now a classical flow, very few velocity data exist because of the limitations of the classical measurement techniques. After demonstrating that the conditions for the two-dimensionality were satisfied, LDV was employed to measure the mean velocity profiles in the configuration shown on Fig. 1. Numerical results were obtained with a full compressible Navier-Stokes solver developed at VKI which uses the implicit factorization algorithm by Beam & Warming [8]; they were in good agreement with the measured values as shown in Fig. 2, except in the upstream boundary layer region where particle lag is important. A full report on the above elements is found in [9, 10 and 11]; a summary has recently been published [12]. An interim report is also available [13].

The 3D interaction will be the principal subject of this report. First, calculations using the 3D version of the compressible Navier-Stokes code developed at the VKI and mentioned above will be summarized. Then the experimental tests will be discussed and the results obtained with LDV will be presented and compared with the numerical results.

2. THE 3D INTERACTION

The test case studied was the skewed or glancing shock wave laminar boundary layer interaction depicted on Fig. 3. Computationally, this interaction represents one of the most severe test cases for a compressible Navier-Stokes solver since it involves both shock waves and separation, two of the most difficult features to accurately predict numerically. In this respect, laminar interactions are better test cases than turbulent interactions since they do not involve uncertainties associated with turbulence modelling. Experimentally, this interaction is also challenging because it is essential to produce accurate flowfield data in regions which, due to wind tunnel size limitations, will be seen to have dimensions of only a few millimeters. LDV is the logical choice, for a measuring instrument, but the 3D configuration, the high speed outer flow, and the need to perform the measurements within a few tenth of a millimeter from the surfaces pose special problems. As mentioned in the introduction, the two latter points were studied in earlier phases of this Grant. Thus, only the 3D nature of the problem was a new aspect.

2.1 Computations with a Navier-Stokes solver

In the numerical part of the research program, the implicit approximate factorization algorithm by Beam & Warming [8] was coded to solve the full compressible Navier-Stokes equations in an arbitrary coordinate system in a way similar to that presented by Pulliam & Steger [14]. The algorithm was chosen both because of its unconditional linear stability property which allows the use of large time steps for fast convergence, and because the truncation error on the steady solution depends only on the grid used. A single flow condition was considered; namely : Mach number, M=2.25; Reynolds number, Re (based on X_F - Fig. 3) = 108 000; X_F=9 cm; and free stream temperature, T_∞=146°K. The wedge angle α was 6°; all details of the computations are discussed in [15] and will not be repeated here. Only a few pertinent results will be shown.

Two meshes were fitted successively in the numerical domain. The first mesh had 35 x 36 points in each of the 20 planes parallel to the flat plate. The typical longitudinal mesh size was approximately 10 boundary layer thicknesses. The second mesh had 25 planes, each of which contained 65 x 49 points, which gave a typical longitudinal mesh size of 5 boundary layer thicknesses. Starting from an initial 2D flow field, the computation converged after 300 time steps on the coarse mesh, i.e., after 100 hours on a Digital VAX 11/780 (18 minutes per time step). Starting from the interpolated coarse mesh solution, the computation converged after 200 time steps on the fine mesh, i.e., 7 hours on a NAS computer.

Figure 4 compares the numerical and experimental results for the skin friction patterns on the flat plate. Figures 4a shows computed surface shear stress vectors (plotted as their cubic root on a part of the numerical domain) for the fine mesh case and figure 4b shows a surface flow visualization (this was obtained with X_F=12 cm). The numerical results are seen to produce a pattern similar to the experiment, in which the skin friction arrows deviate away from the wedge far upstream of the inviscid shock wave. In figure 4b, the boundary between the upstream region covered by the visualizing substance and a region devoid of it is interpreted as a line of separation. It is impossible from the discrete numerical results to draw such a line but the herringbone pattern of the skin friction arrows is a strong indication of the presence of separation. Further, on the fine mesh, the dual herringbone pattern suggests the presence of a secondary separation. The numerical results also confirm the conical nature of the interaction footprint. In the experimental visualization, the conical region is limited outboard due to finite shock generator size effects (trailing edge expansion) whereas no such problem exists in the computation and the conical region is seen to cover the whole domain shown. The conical nature of the surface flow field also appears on Fig. 5 which shows the isobars on the flat plate (fine mesh). These appears as rays emanating from a single point (conical origin) in the major part of the numerical domain.

Due to the conical nature of the interaction footprint, plane cuts of the flow field were performed normal to the inviscid shock wave and to the plate. The velocity vector was projected on such planes and the cross flow Mach number was computed. Cross flow Mach number contours are shown on Fig. 6 & 7 on planes at L_{SH}/X_F=0.5 and 1.5. They show the existence of a low cross flow velocity region beneath the shock, due to the separation of the boundary layer. The vertical extent of the interaction region is seen to be very small, in contrast to the large extent of the interaction footprint (Figs. 4 & 5). The interaction is seen to cause a mere bulge in the boundary layer edge.

Observing figs. 6 & 7 one notices that not only the size of the interaction footprint increases when progressing outboard from the wedge but also the height of the interaction region. It was concluded that self-similarity exists in the vertical direction.

To identify the existence of a vortical structure in the interaction, the streamwise vorticity was computed on the fine mesh. Contours of this quantity are shown in Fig. 8 in the cut plane at L_{SH}/X_F=1.5. The major part of the flow field is seen to exhibit a very small streamwise vorticity meaning either that the flow is irrotational (main outer flow) or that the vorticity is essentially transverse as in the incoming boundary layer. However, three regions of important streamwise vorticity do appear. The larger one is a zone of positive (clockwise) vorticity associated with the separation of the incoming boundary layer : it is the primary vortical structure. Beneath it, there exists a small region of negative vorticity, the secondary vortical structure, associated with the secondary separation observed in Fig. 4. Finally, one also observes a zone of negative vorticity in the corner of the wedge and plate. This is called the corner vortex. Its intensity is seen to be smaller than that of the main vortex, at least for this flow condition.

The measured pressure distributions on the flat plate were compared with the results of the computation on both meshes. The comparison is shown in Fig. 9 for $y/X_F=5/9$. The pressure is normalized by the minimum pressure in the distribution and the abscissa is the dimensional x-coordinate. One first notices that the overall pressure rise is smaller in the experiment than in the computation. This is due to an experimental Mach number lower than foreseen. This appeared clearly in a repeat run of the experiments in which the true Mach number was found to be 2.15. Otherwise, the agreement between measured and computed pressure distributions is seen to be poor for the coarse mesh and improved for the finer mesh, although some discrepancies still exist. This is not surprising since the typical longitudinal mesh spacing is still approximately five boundary layer thicknesses. The numerical results on the fine mesh do not represent a spatially converged solution and therefore the physical information which can be extracted from it must be considered with caution.

Finally, longitudinal (x-component) velocity distributions were computed at four locations downstream of the leading edge; they are plotted in Fig. 10. As they differ markedly, one from the other, it is apparent that a measurement of the velocity profiles at the same stations under identical conditions would represent a significant check on the computational results.

In summary, an implicit approximate factorization algorithm for solving the compressible Navier-Stokes equations has been successfully coded to obtain a solution of the skewed shock wave laminar boundary layer interaction. The numerical solution reproduces the essential features of the flow. It indicates :

1. the separation of the boundary layer which produces an elongated vortical structure beneath the outer shock wave;

2. the conical nature of the interaction footprint as shown by the ray-like aspect of the isobars on the flat plate;

3. that the comparison between experimental and computed pressure distributions is satisfactory, taking account of the limitations of the mesh used;

4. that a measurement of the longitudinal component of the velocity would represent an important step in validating the codes;

2.2 Experimental results with LDV

To validate the computations described earlier, it was proposed to perform complementary LDV measurements of the mean longitudinal (x-direction) velocity distributions within the boundary layer at several characteristic positions upstream and downstream of the shock.

Since earlier LDV tests in a two-dimensional shock/boundary layer interaction flow revealed difficulties which could be attributed to the velocity lag which the seeding particles develop when passing through steep velocity gradients [9, 16], further experiments were conducted to increase the sensitivity of the LDV system so that smaller seeding particles can be observed and the signals of large particles can be rejected and to improve the size distribution of the seeding particles by developing a particle generator producing particles with a narrower size distribution.

The experience gained by these studies was very helpful for the execution of the velocity measurements.

2.2.1 Experimental set-up

The measurements were conducted in the S1 wind tunnel of VKI. This is a continuous closed circuit facility with a 40 cm x 40 cm test section and a nominal free stream Mach number M_∞=2.25. Stagnation pressure was kept close to 0.1 bar giving a unit Reynolds number of about 10^6 per meter.

The model consisted of a flat plate with a sharp leading edge and a 15 cm high wedge normal to it which was set at an angle of incidence of $\alpha=6°$, acting as shock generator (see Fig. 3). Details are given in [6, 11, 15, 17]. An optical glass plate was inserted in the lower part of the wedge so that LDV measurements in the forward scattering mode were feasible with the receiving optics of the LDV system looking through the wedge. Figure 11 is a photograph of the model, with its windows, installed in the S-1 wind tunnel.

The LDV set up, Fig. 12, operates in the forward scattering mode. Probe volume size was minimized using a collimator, beam spacer and beam expander and a 100 μm pinhole giving a computed probe volume width of 0.09 mm and length of 1,7 mm. The number of fringes was 17 and the fringe spacing was 5.2 μm.

A TSI 1990A counter type signal processor was used to evaluate the Doppler signal. A Commodore computer with extension unit and floppy disk drive provided the possibility to store the LDV data on tape for off-line processing on the VKI VAX 11/780 computer and to obtain an on-line mean value and standard deviation of each measured velocity. For each velocity measurement, 1024 samples were taken. Seeding was found to be essential for adequate data rates; a Norgren "micro-fog", atomizer was employed with Shell Ondina Oil (number 15) yielding a mean particle size of 2.0 μm as demonstrated with the classic oblique shock technique. The TSI 1990A provides the possibility of rejecting signals from large particles by an adjustable signal amplitude limiter.

2.2.2 Experiments

Velocity profiles were measured at the axial stations X=85,3 mm, 203,7 mm and 350,9 mm from the leading edge of the flat plate at a lateral distance Y=90 mm from the apex of the shock generator. These positions, and the predicted normalized velocity profiles from the code discussed in 2.1 are presented in Fig. 10.

No measurements were made at station £4 , X=492,9 mm, downstream of the interaction region, because of the lesser importance of this point and because of the fact that a significant modification of the model support would have been necessary to move the model upstream in order to align this position with the windows of the wind tunnel.

Thorough cleaning of the model surfaces and the windows was mandatory before each measurement to obtain a suitable signal/ noise ratio. Also, before each test the LDV system was checked at low flow velocity and was readjusted if necessary. After reducing the tunnel pressure to working conditions and accelerating to full wind speed total pressure p_t, static pressure p_∞ and total temperature T_t were determined and the free stream Mach number M_∞ calculated. It was usually slightly lower (2.15) than the nominal M_∞=2.25 value.

Several LDV measurements were made at each measuring position with different settings of the amplitude limiter, amplifier gain and filter bandwidth to obtain some information on the influence of these parameters. From the 1024 samples used for each velocity measurement, the mean value and the standard deviation of the velocity were computed on line by the Commodore computer. Thus it was possible to obtain some evidence of the validity and accuracy of the individual measurement during each test. Besides this online data evaluation, the measured data were stored on cassette tape for later processing on the VKI VAX 11/780 computer.

Velocity histograms and mean velocity and standard deviation for each measuring position were calculated on the VAX; the results were practically a duplication of the calculations already made on the Commodore computer. This enabled a cross check to be made on the results which was helpful because of slight differences in the respective computer codes. The histogram plots gave very valuable information on the validity of the individual measurements and on the accuracy of the mean velocity values. As

an example, Fig. 13 is a histogram near the outer edge of the boundary layer and can be characterized as relatively "sharp". The difference between the peak (maximum) velocity and the mean velocity is only 2%. Figure 14 shows the influence of the amplitude limiter for a point deep within the boundary layer where the larger particles are expected to be traveling much faster than the smaller ones. In Fig. 14a, the large high velocity "tail" is quite apparent and an important difference exists between the peak and mean velocities recorded. Fig. 14b illustrates the extend to which the amplitude limiter has reduced the skewness due to the large particles. In the mean velocity results to be discussed later, only data obtained with the amplitude limiter in operation are presented; e.g., results from the data of Fig. 14a would not be analyzed.

2.2.3 Results

For each test, the measuring positions, the TSI counter settings, data rate, velocities and standard deviations of each measuring run were recorded. Velocities presented are :

U_{peak} : velocity value of the peak of the histogram;

U_{mean} : Mean velocity obtained from the histogram

Velocity profiles for the three X-positions X=85.3 mm, X=203.7 mm and X=350.9 mm are presented in comparison with the predicted profiles in Fig. 15 to Fig. 17. On each figure, Z=0 refers to the observed probe volume position on the plate surface as determined by the merging of the two laser beam spots into one spot. The accuracy in the determination of the Z=0 point is not very good and the data were corrected by an amount ΔZ to force agreement between the measured and predicted values. As will be seen, the corrections always had a negative sign indicating a systematic error. The corrections were never more than 0.5 mm and experience with LDV measurements near solid surfaces [7] suggests

that this is reasonable.

Data for which the standard deviation σ was greater than 75m/s were arbitrarily rejected. The velocities are normalized with the free stream velocity measured with the LDV :

U_∞=538 m/s for U_{peak}

U_∞=527 m/s for U_{mean}

The average free stream velocity calculated from the total temperature and pressure ratio p_∞/p_t was U_∞=540 m/s ± 8 m/s. This is very close to the free stream velocity obtained with U_{peak} (538 m/s). The lower value 527 m/s obtained for the mean velocity U_{mean} is due to the inherent error in the calculation of mean values from skewed distributions.

Results for station 1 : X=85,3 mm; upstream of interaction.

Figure 15a shows the velocity profiles obtained, on different days, for U_{peak}. A very good agreement with prediction is obtained by correcting the Z coordinate by ΔZ=-0,2 mm, as shown in Fig. 15b. This correction is clearly justified in this case of an attached laminar boundary layer since the velocity should be essentially linear in the wall region and must go to zero at the wall.

The mean velocities from the same data are shown in Fig. 15c; a ΔZ correction of -0,2 mm again seems a reasonable choice as shown in Fig. 15d. It should be noted that there is no essential disagreement between the profile obtained with mean values or peak values, particularly in the important region of high gradients.

Results at station 2 : X=203,7 mm; separated flow region.

Figure 16a shows the peak velocity results in comparison with

the theoretical prediction. A correction with $\Delta Z=-0,5$ mm is shown in Fig. 16b; superimposed are the results for the corrected mean velocities which are in reasonable agreement. The general shape of the theoretical prediction in the separated flow region is reproduced by the experimental results.

Results at station 3 : X=350,9 mm; reattachment region.

Figure 17 shows the velocity profile in the reattachment region; a correction of $\Delta Z=-0.25$ mm has been applied. Good agreement between the mean and peak velocities is again observed and the theoretical profile is well matched in this region of very large gradients.

3. DISCUSSION OF THE RESULTS

An analysis of all the experimental results shows that :

a) repeatability of a velocity measurement at a given station from one day to the next was typically ±3% and was never worse than ±7%;

b) agreement between peak and mean values of the normalized velocity was, on average, within ±5% when the amplitude limiter was employed to reject signals from the largest particles;

c) the overall accuracy of the measured velocity profiles is approximately ±5% based largely on the excellent agreement between theory and experiment in a region (station 1) which is a simple attached compressible boundary layer.

4. CONCLUSIONS

The following conclusions are drawn from this study :

- The level of agreement between the LDV measurements and the theoretical prediction from the Navier-Stokes solver based on the Beam & Warming algorithms is sufficient to state that the code has been validated in this severe test case of a 3D shock wave-laminar boundary layer interaction.

- A set of experimental data with an overall accuracy of ±5% characterizing a sensitive fluid dynamic variable in a 3D separated flow, the axial component of the velocity, is now available for comparison with other numerical predictions.

5. REFERENCES

1. PEAKE, D.J.: Three dimensional swept shock/turbulent boundary layer separation with control by air injection.
   Ph.D. Thesis, Carleton University, Ottawa, 1975.

2. OSKAM, B.: Three dimensional flow fields generated by the interaction of a swept shock with a turbulent boundary layer.
   Princeton University, Gas Dynamics Lab., Report 1313, December 1976.

3. KUBOTA, H. & STOLLERY, J.L.: An experimental study of the interaction between a glancing shock wave and a laminar boundary layer.
   Journal of Fluid Mechanics, Vol. 116, March 1982, pp 431-458.

4. DOLLING, D.S. & BOGDONOFF, S.M.: Blunt fin induced shock wave turbulent boundary layer interactions.
   AIAA Journal, Vol. 20, No 12, December 1982, pp 1674-1680.

5. DEGREZ, G. & GINOUX, J.J.: Surface phenomena in a three dimensional skewed shock wave laminar boundary layer interaction.
   AIAA Journal, Vol. 22, No 12, December 1984, pp 1764-1768;
   also von Karman Institute Preprint 1983-04.

6. GINOUX, J.J. & DEGREZ, G.: Three dimensional skewed shock wave boundary layer interaction : laminar and turbulent behaviour.
   AFOSR Final Scientific Report, Grant AFOSR 82-0051, December 1982; also von Karman Institute CR 1983-05/AR.

7. DEGREZ, G. & GINOUX, J.J.: Velocity measurements in a three dimensional shock wave laminar boundary layer interactions. Part 1 - Low speed 2D LDV measurements.
   Interim Scientific Report, AFOSR Grant 83-0273, September 1984; also von Karman Institute CR 1984-29.

8. BEAM, R.M. & WARMING, R.F.: An implicit factored scheme for the compressible Navier-Stokes equations.
   AIAA Journal, Vol. 16, No 4, April 1978, pp 393-402.

9. BOCCADORO, C.H. & WENDT, J.F.: Investigation of an oblique shock wave laminar boundary layer interaction using LDV.
   AFOSR Scientific Report, AFOSR Grant 83-0273, June 1984;
   also von Karman Institute TN 152, June 1984.

10. DEGREZ, G.; BOCCADORO, C.H.; WENDT, J.F.: LDV velocity measurements in thin laminar boundary layers, separated and unseparated, and comparison with numerical computations.
    ICAS Paper 84-2.3.1.; also von Karman institute Preprint 1984-16.

11. DEGREZ, G.: Etude théorique et expérimentale d'intéractions bi et tri-dimensionnelles entre ondes de choc et couches limites laminaires.
Ph.D. Thesis, Université Libre de Bruxelles, 1984.

12. DEGREZ, G.; BOCCADORO, C.H.; WENDT, J.F.: The interaction of an oblique shock wave with a laminar boundary layer revisited. An experimental and numerical study.
Journal of Fluid Mechanics, Vol. 177, pp 247-263, 1987.

13. DEGREZ, G. & GINOUX, J.J.: Velocity measurements in a 3D shock wave laminar boundary layer interaction.
Part 2 - High speed 2D LDV measurements.
Interim Scientific Report, AFOSR Grant 83-0273, September 1985; also von Karman Institute CR 1985-24.

14. PULLIAM, T.H. & STEGER, J.L.: Implicit finite difference simulation of three-dimensional flow.
AIAA Journal, Vol. 18, No 2, February 1980, pp 159-167.

15. DEGREZ, G.: Computation of a three-dimensional skewed shock wave laminar boundary layer interaction.
AIAA Paper 85-1565; also von Karman Institute Preprint 1985-22.

16. SCHÜTZ, W.: Effect of seeding particle size on LDV measurements in a compressible boundary layer.
AFOSR Scientific Report, AFOSR Grant 83-0273, June 1985; also von Karman Instiute PR 1985-06, June 1985.

17. DEGREZ, G.; GROSCHE, F.; WENDT, J.F.: The three-dimensional shock wave boundary layer interaction : experiment and theory.
To be submitted in the J. of Fluid Mechanics, 1987.

APPENDIX A

Chronological bibliography of all publications resulting from the research

1. DEGREZ, G.; BOCCADORO, C.H.; WENDT, J.F.: LDV velocity measurements in thin laminar boundary layers, separated and unseparated, and comparison with numerical computations.
ICAS Paper 84-2.3.1.; also von Karman institute Preprint 1984-16.

2. BOCCADORO, C.H. & WENDT, J.F.: Investigation of an oblique shock wave laminar boundary layer interaction using LDV.
AFOSR Scientific Report, AFOSR Grant 83-0273, June 1984;
also von Karman Institute TN 152, June 1984.

3. DEGREZ, G.; BOCCADORO, C.H.; WENDT, J.F.: The interaction of an oblique shock wave with a laminar boundary layer revisited. An experimental and numerical study.
Journal of Fluid Mechanics, Vol. 177, pp 247-263, 1987.

4. DEGREZ, G.: Etude théorique et expérimentale d'interactions bi- et tri-dimensionnelles entre ondes de choc et couches limites laminaires.
Ph.D. Thesis, Université Libre de Bruxelles, 1984.

5. DEGREZ, G.; GROSCHE, F.; WENDT, J.F. : The three-dimensional shock wave boundary layer interaction : experiment and theory.
To be submitted for publication in the Journal of Fluid Mechanics, 1987.

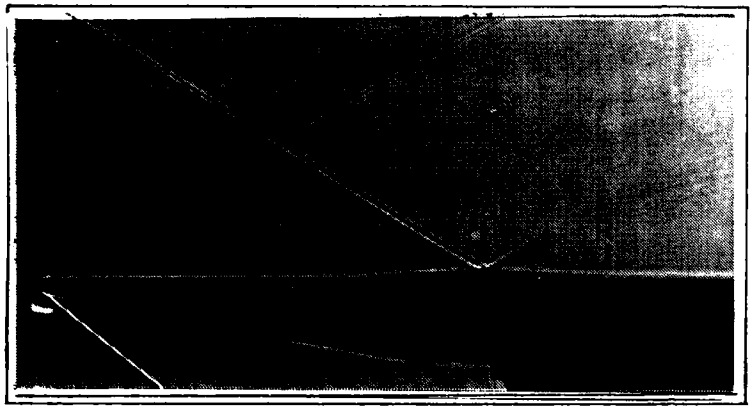

$M_\infty = 2.20$
$Re_{Xsh} = 1.12 \times 10^5$
Xsh = 80 mm

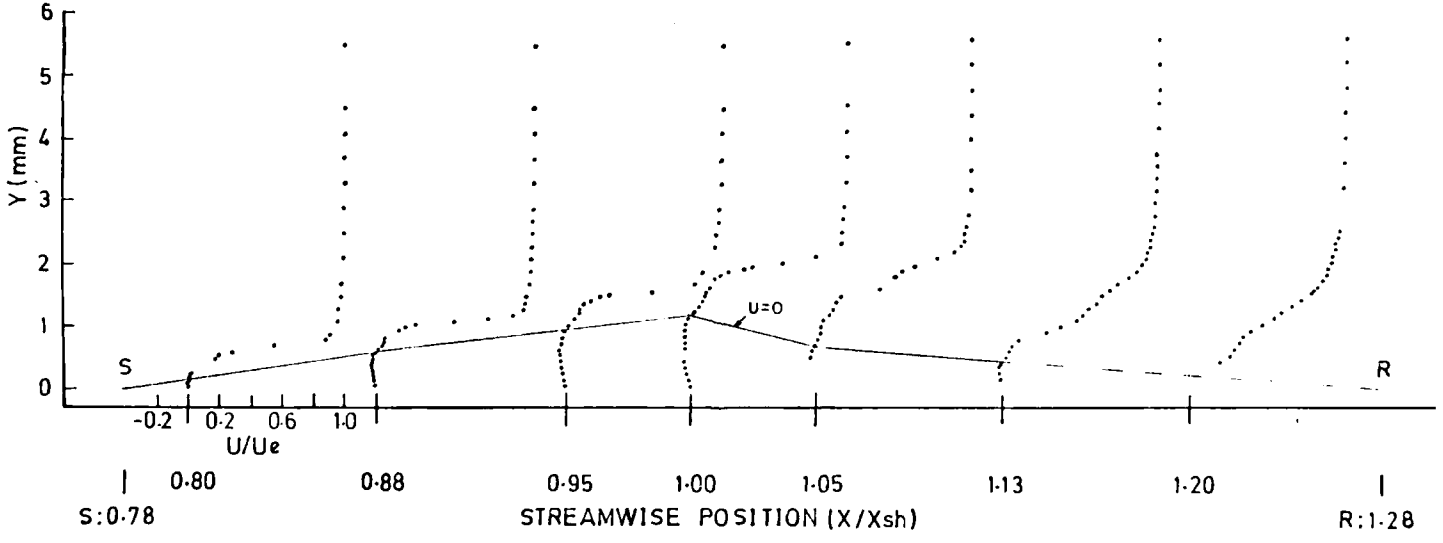

Fig. 1 - Mean velocity profiles in separated region of a 2D interaction

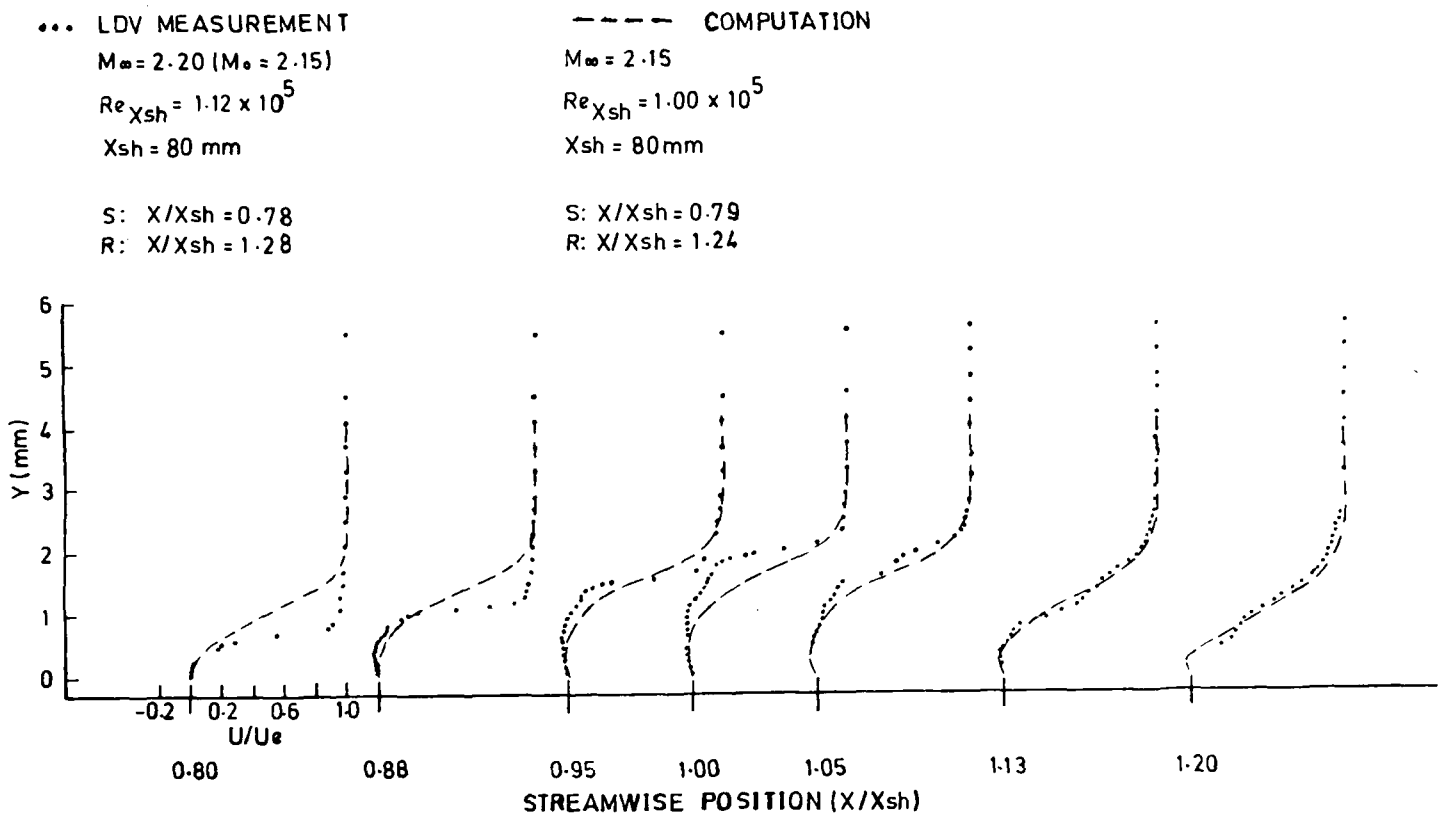

Fig. 2 - Comparison of computed and measured velocity profiles in separated region.

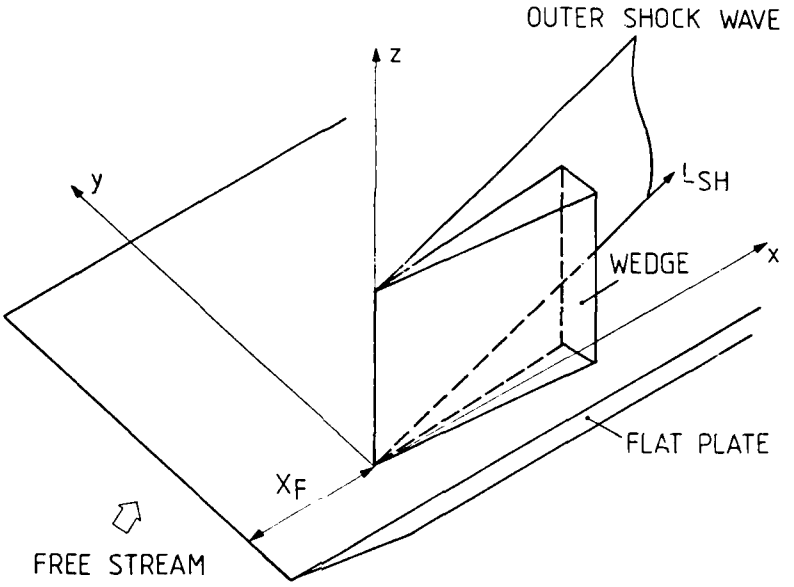

(a) PERSPECTIVE VIEW

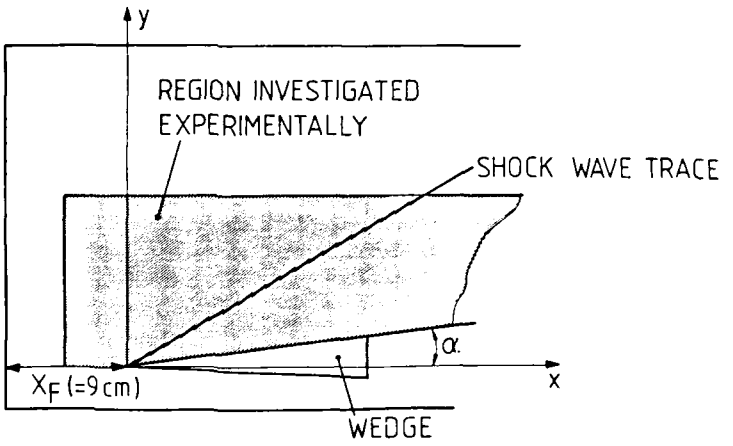

(b) VIEW FROM ABOVE

Fig. 3 - Schematic of the flow field configuration.

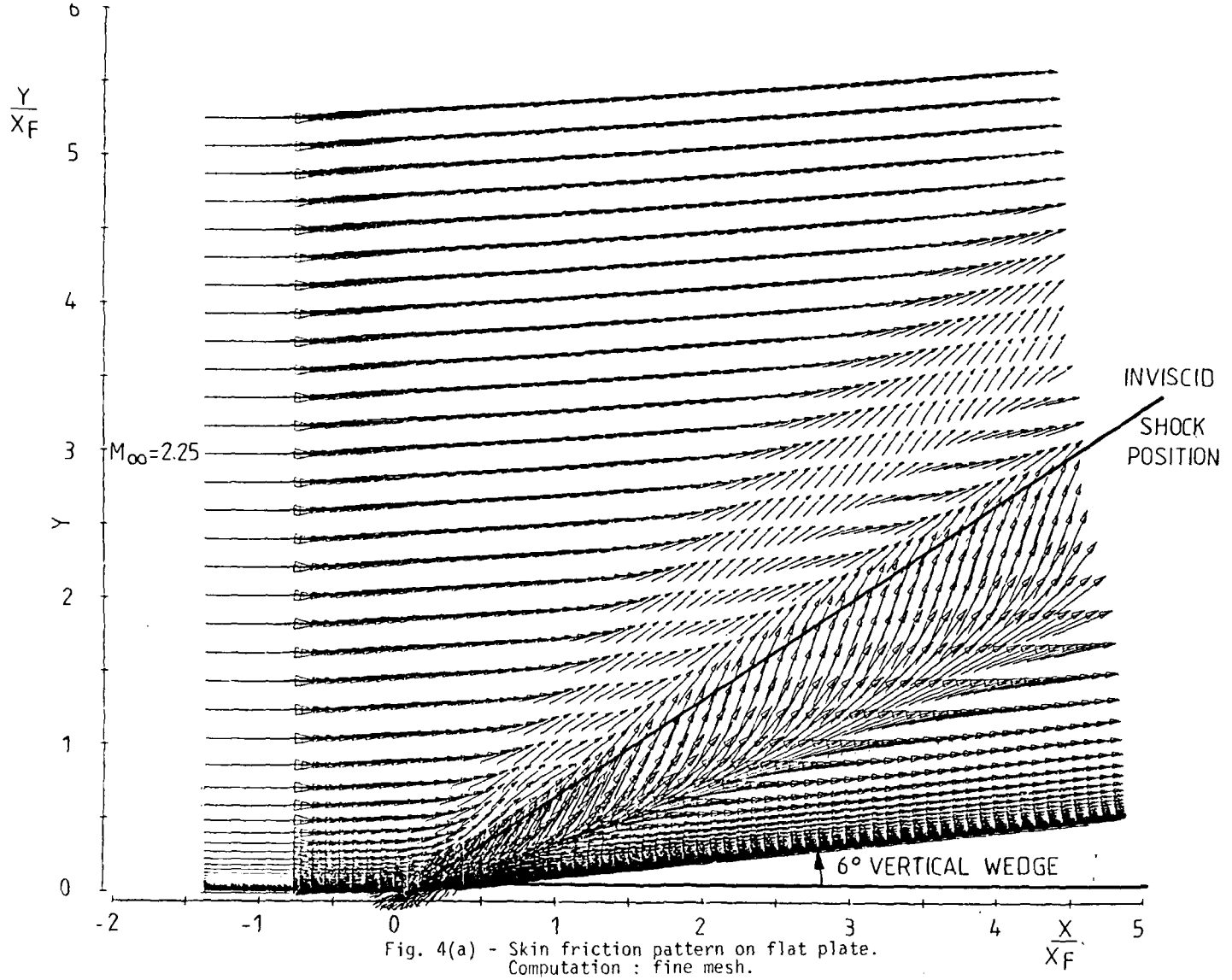

Fig. 4(a) - Skin friction pattern on flat plate.
Computation : fine mesh.

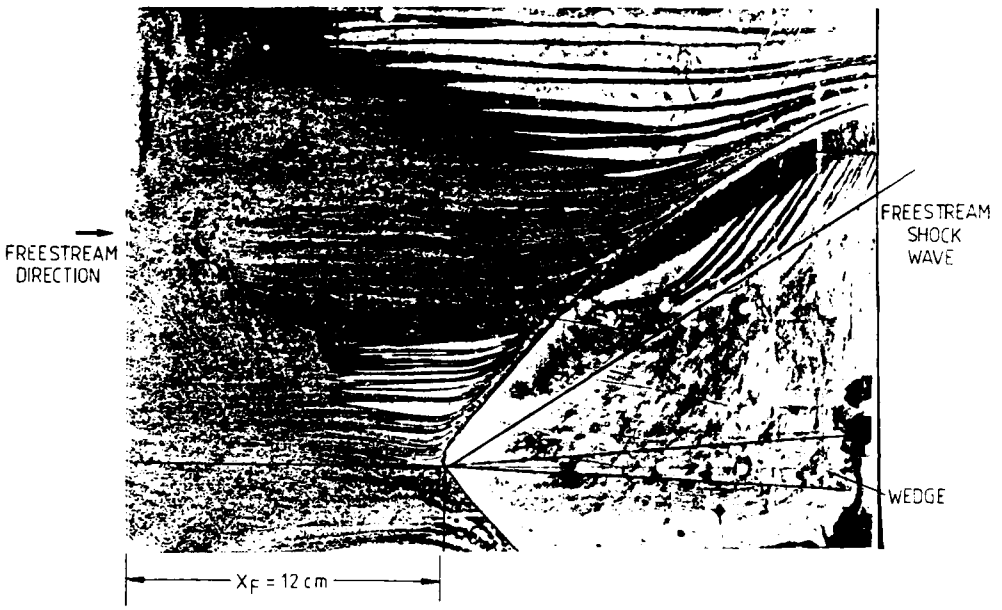

Fig. 4(b) - Skin friction pattern on flat plate.
Experiment : surface flow visualization.

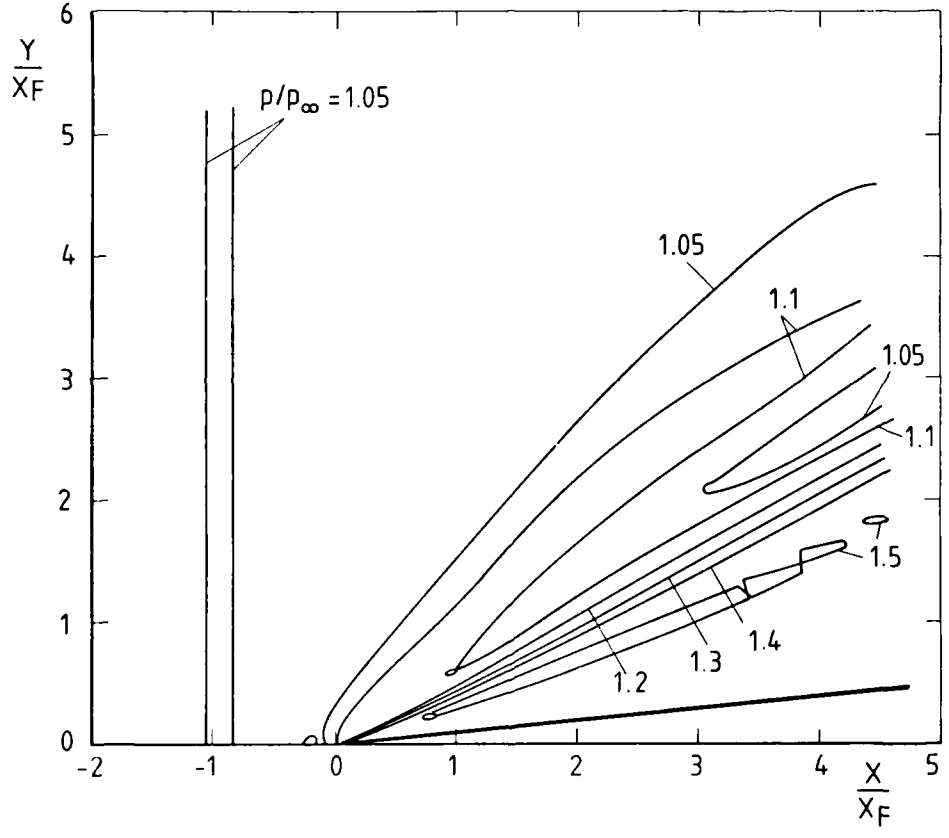

Fig. 5 - Isobars on flat plate.

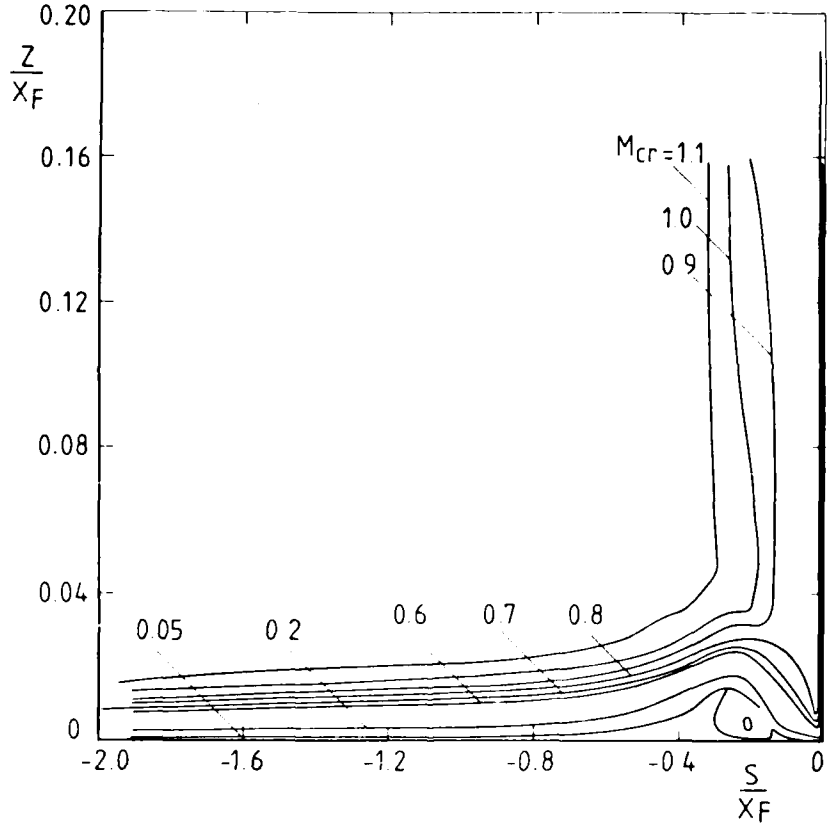

Fig. 6 - Cross flow Mach number contour on cut plane at L_{SH}/X_F= 0.5.

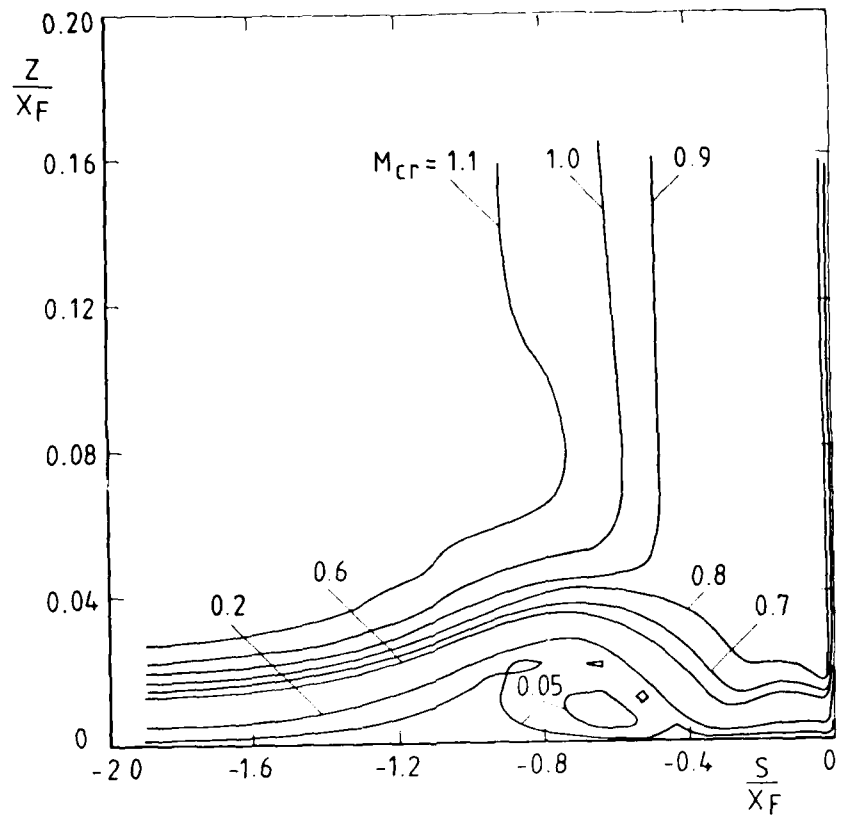

Fig. 7 - Cross flow Mach number contour on cut plane at $L_{SH}/X_F = 1.5$.

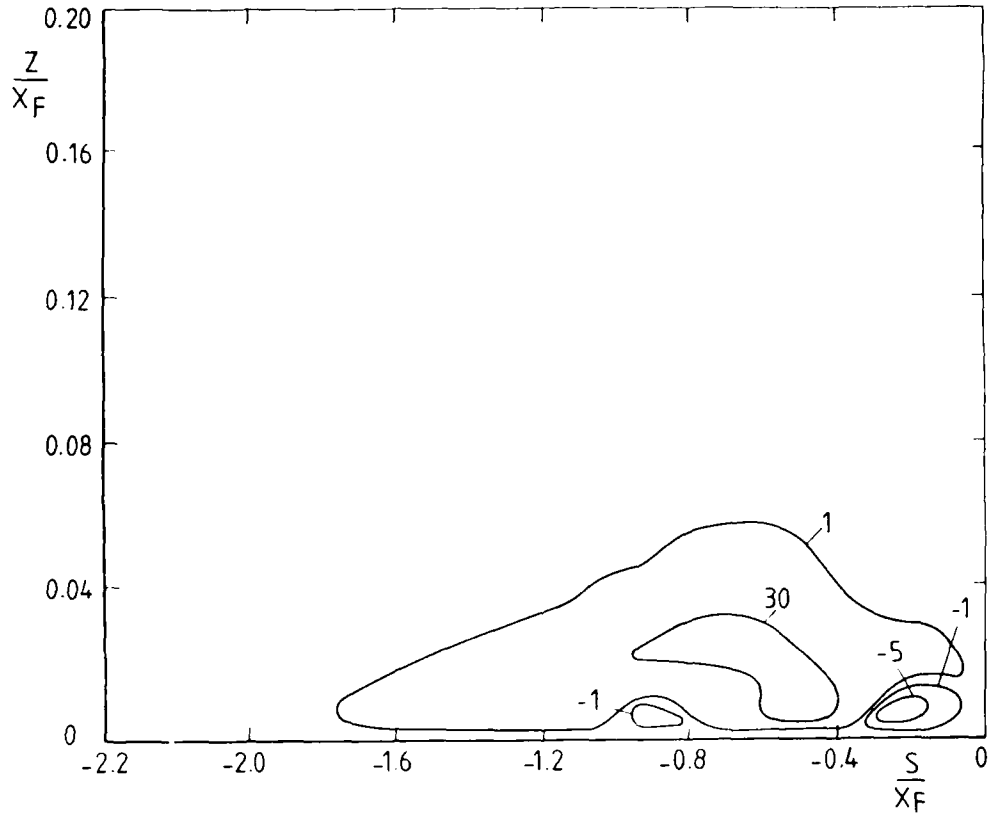

Fig. 8 - Streamwise vorticity contour on cut plane at L_{SH}/X_F= 1.5.

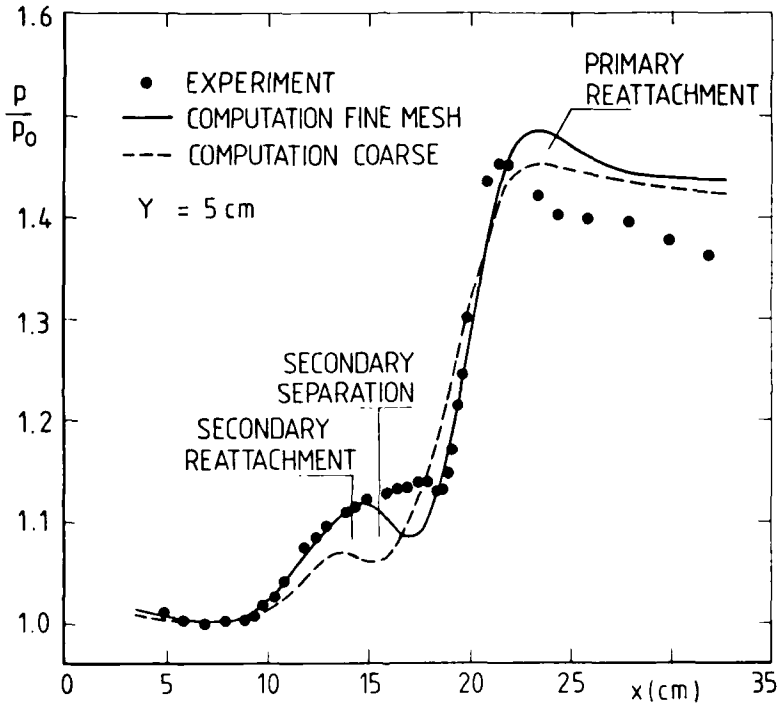

Fig. 9 - Comparison of measured and computed plate pressure distribution at Y=5 cm.

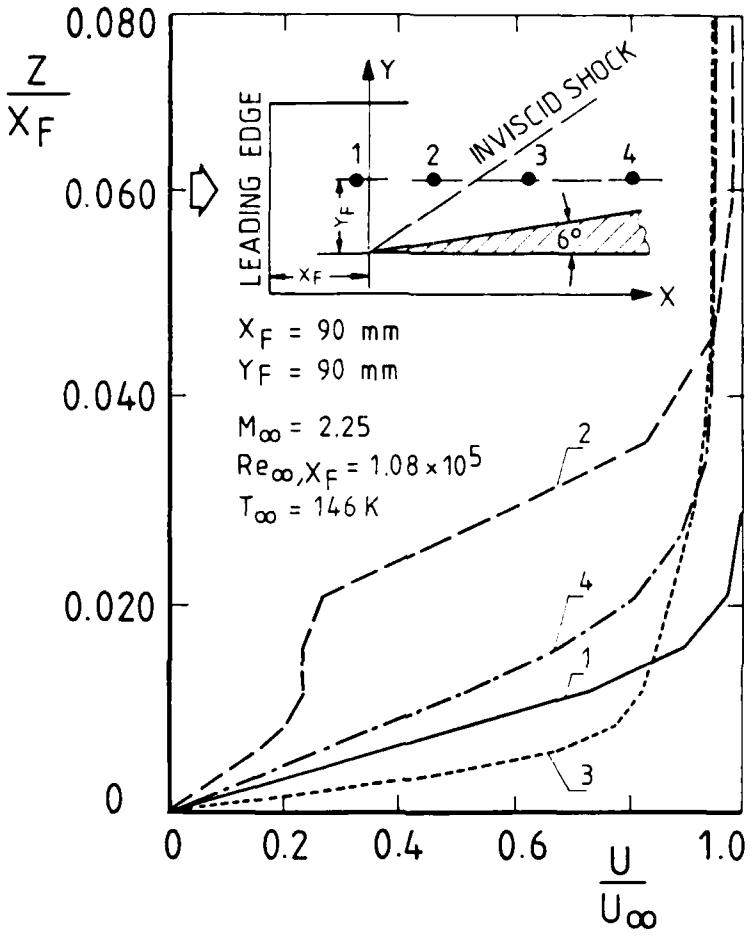

1) UPSTREAM OF INTERACTION, X = 85.3 mm
2) IN SEPARATED ZONE, X = 203.7 mm
3) AT REATTACHMENT, X = 350.9 mm
4) DOWNSTREAM OF INTERACTION, X = 492.9 mm

Fig. 10 - Computed streamwise velocity profiles along a longitudinal cut in the 3D interaction.

Fig. 11 - FLAT PLATE, VERTICAL WEDGE MODEL IN S-1 TUNNEL.
Note windows at base of wedge for LDV.

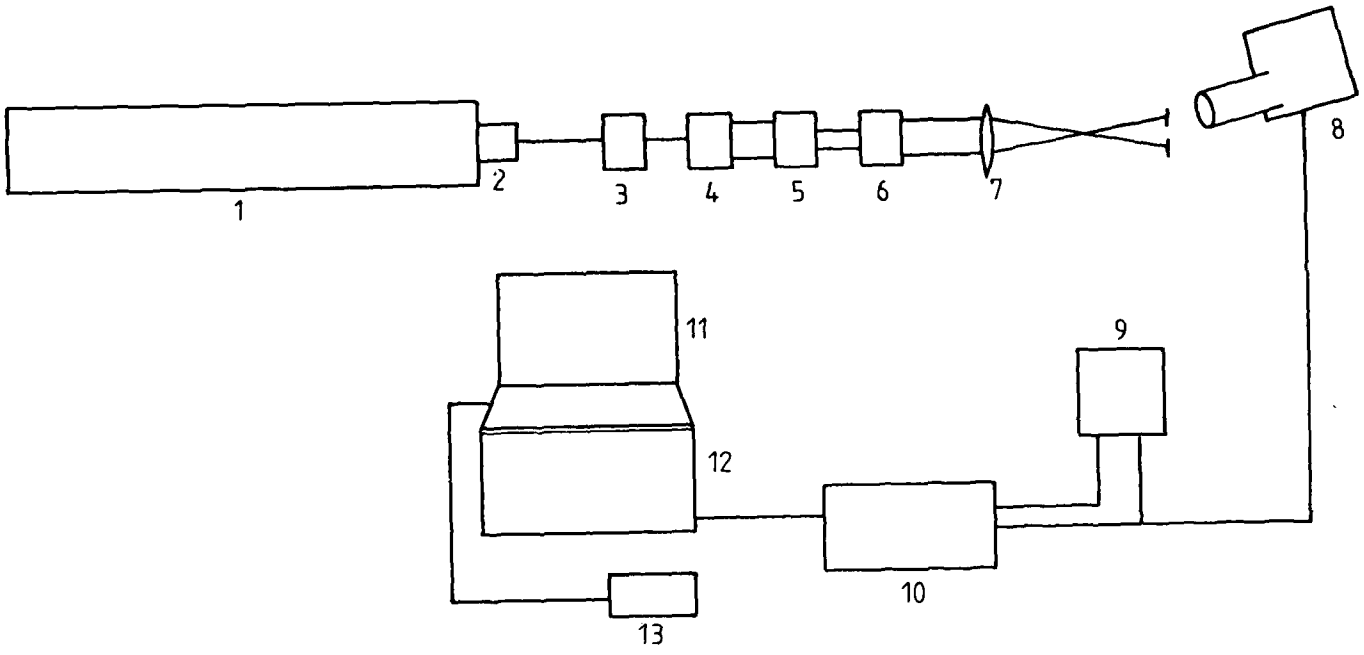

1) SPECTRA PHYSICS 165 ARGON-ION LASER (5 WATTS)
2) COLLIMATOR
3) POLARIZER
4) BEAM SPLITTER (50mm)
5) BEAM SPACER (REDUCER)
6) BEAM EXPANDER
7) LENS (0.5m FOCAL LENGTH)
8) PHOTOMULTIPLIER (RCA 4526)
9) OSCILLOSCOPE
10) TSI COUNTER (1990)
11) COMMODORE COMPUTER (3032)
12) COMMODORE EXTENSION UNIT (# 002)
13) COMMODORE FLOPPY DISK DRIVE (2031)

Fig. 12 - LDV set-up.

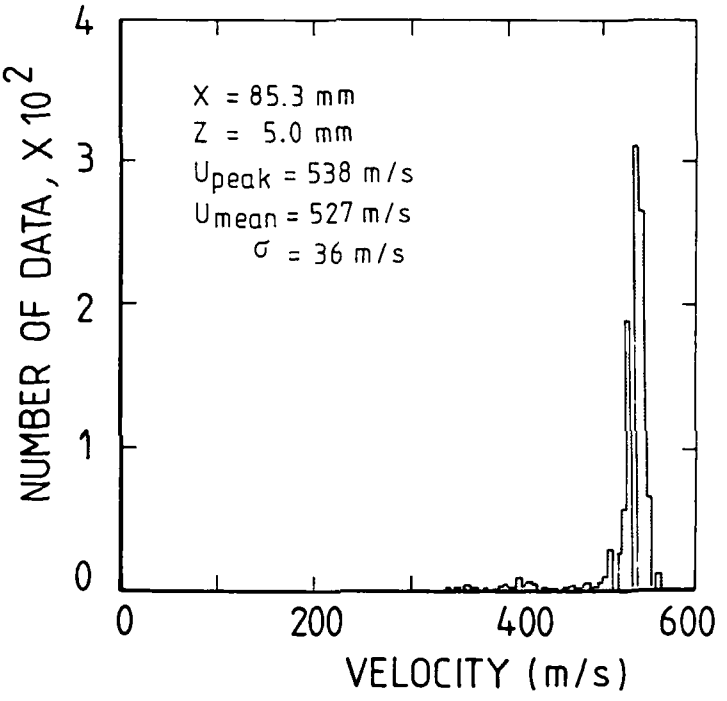

Fig. 13 - Histogram at outer edge of attached boundary layer. Station 1.

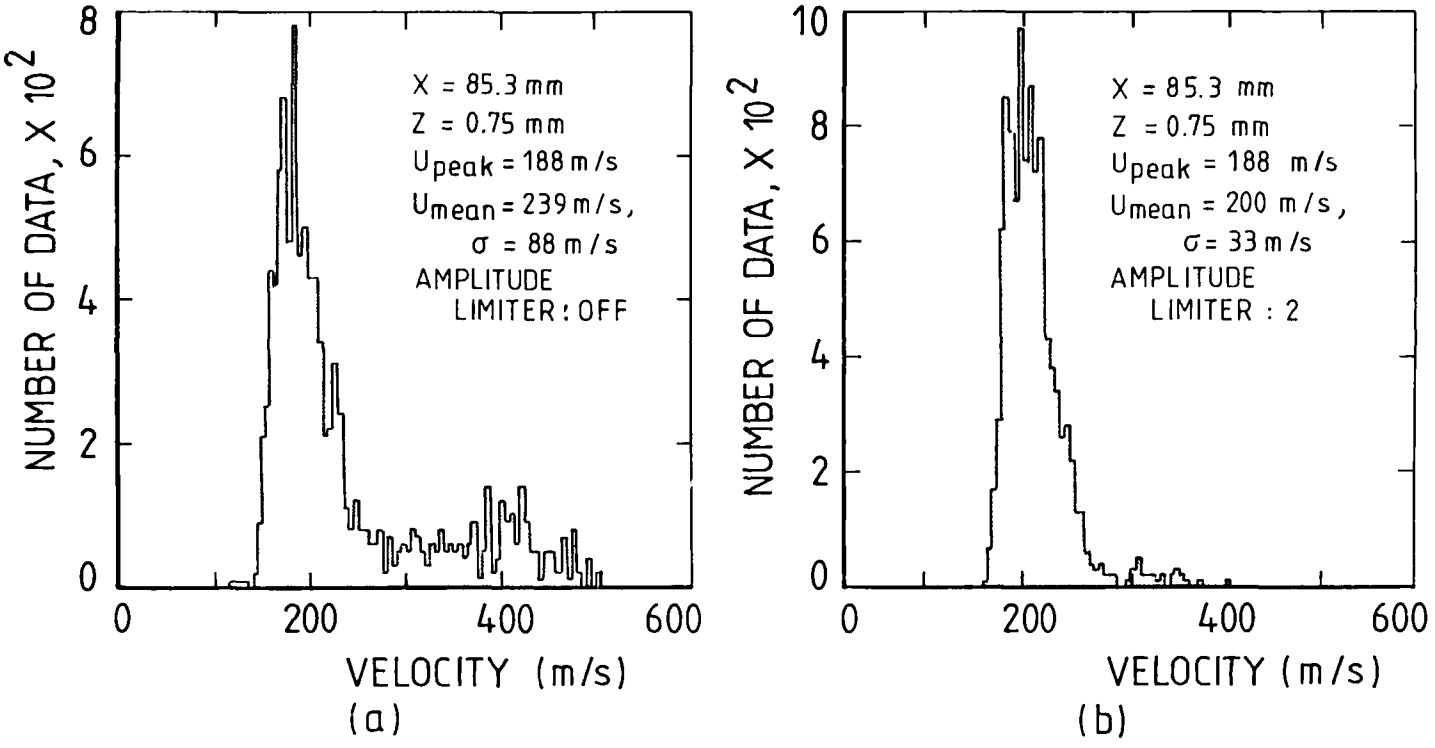

Fig. 14 - Histogram deep within attached boundary layer showing influence of amplitude limiter.

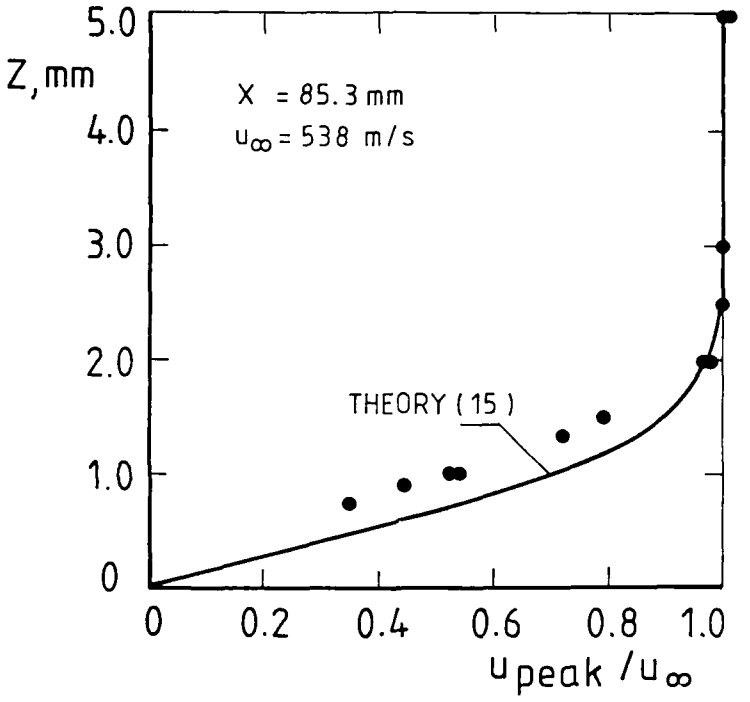

Fig. 15(a) - Raw data : Station 1. Peak velocity.

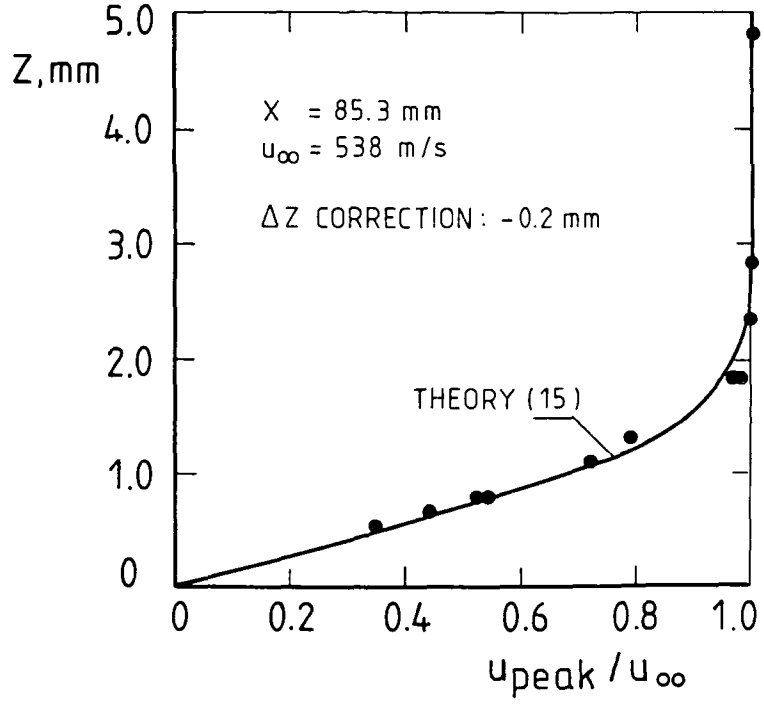

Fig. 15(b) - Corrected data : Station 1. Peak velocity.

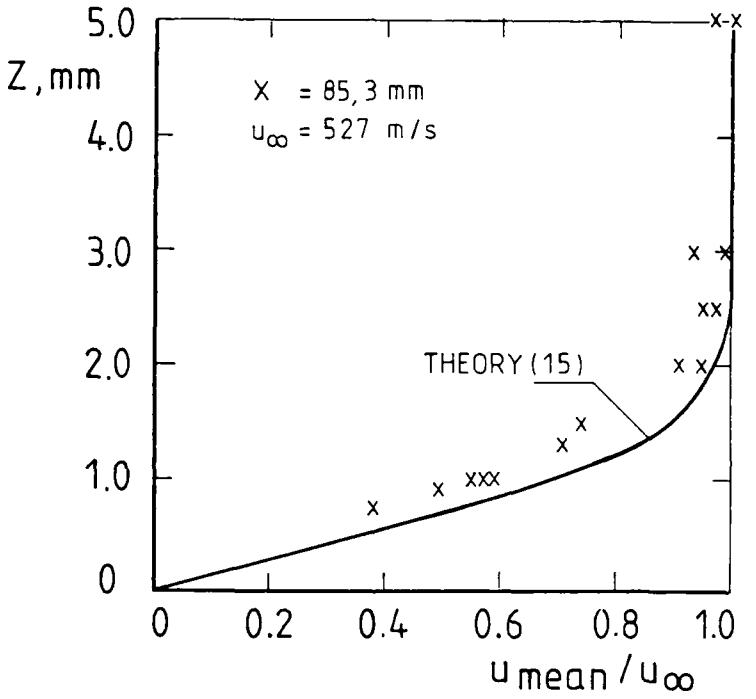

Fig. 15(C) - Raw data : Station 1. Mean velocity.

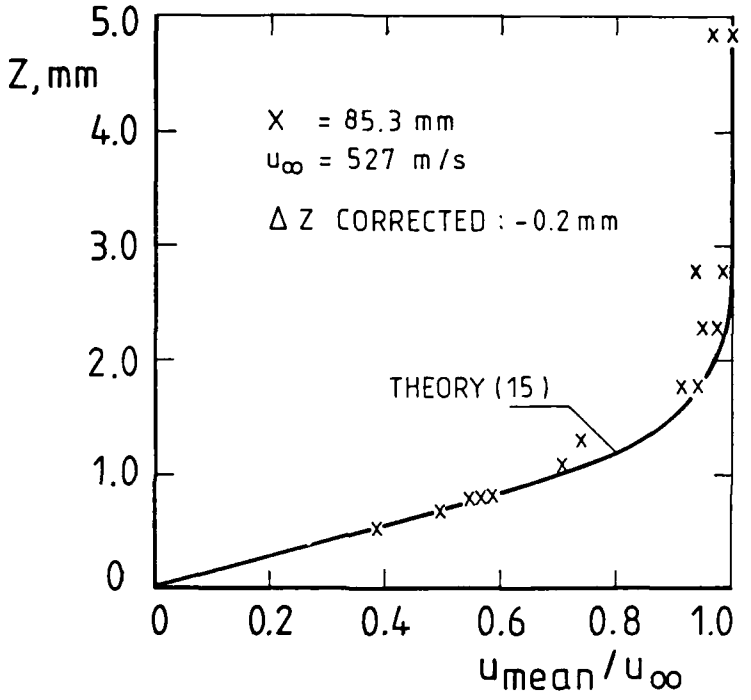

Fig. 15(d) - Corrected data : Station 1. Mean velocity.

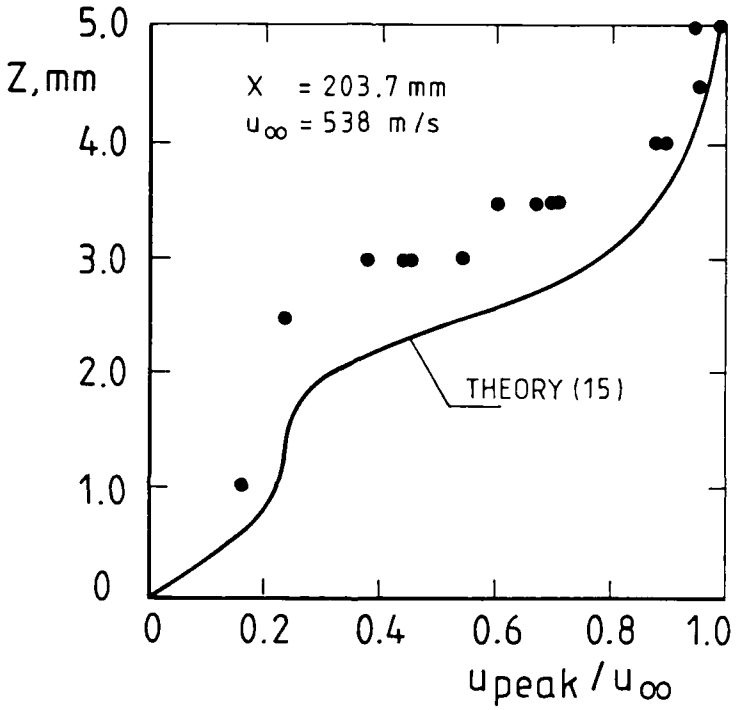

Fig. 16(a) - Raw data : Station 2. Peak velocity.

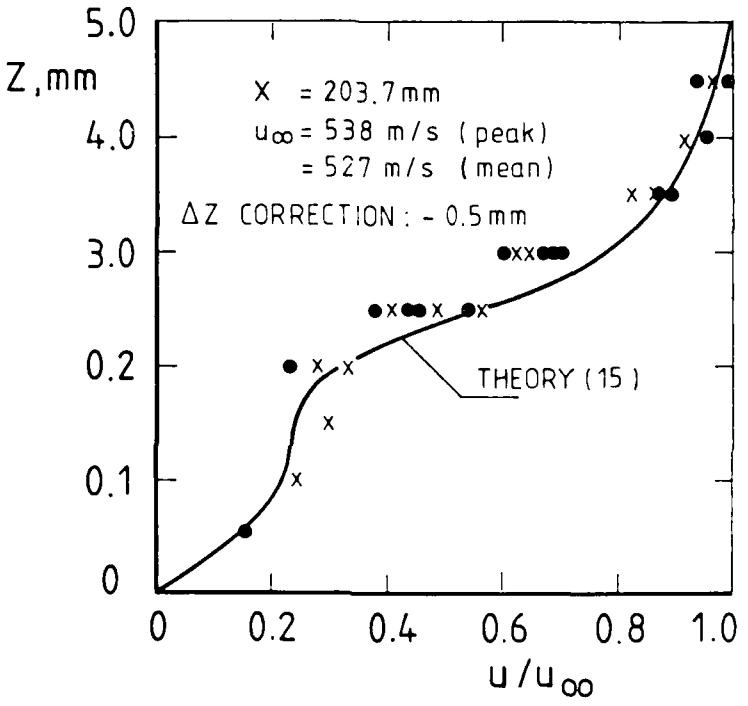

Fig. 16(b) - Corrected data : Station 2.

Peak velocity •

Mean velocity x

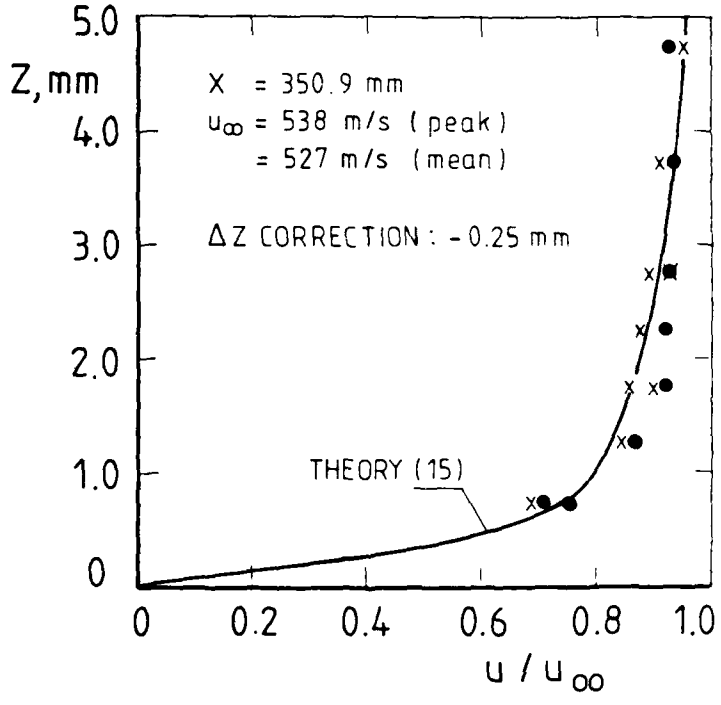

Fig. 17 - Corrected data : Station 3.

Peak velocity •

Mean velocity x

END

DATE
FILMED

2 88

DTIC